EXTENSION OF THE UNSTRUCTURED ALGORITHMS OF LIOU AND STEFFEN JR. AND OF RADESPIEL AND KROLL TO SECOND ORDER ACCURACY EMPLOYING LINEAR RECONSTRUCTION AND APPLICATION TO THE EULER EQUATIONS IN 2D - RESULTS

Edisson Sávio de Góes Maciel, edissonsavio@yahoo.com.br
Mechanical Engineer / Researcher – Rua Demócrito Cavalcanti, 152 – Afogados – Recife – PE – Brazil – 50750-080

Abstract. *In the present work, the Liou and Steffen Jr. and the Radespiel and Kroll schemes are implemented, on a finite volume context and using an upwind and unstructured spatial discretization, to solve the Euler equations in the two-dimensional space. Both schemes are flux vector splitting ones. These schemes are implemented in their second order accuracy versions employing the reconstruction linear method of Barth and Jespersen and their results are compared with their first order accuracy versions and with theoretical results. Five nonlinear flux limiters are studied: Barth and Jespersen (minmod like), Van Leer, Van Albada, Superbee and β-limiter. The time integration uses a Runge-Kutta method of five stages and is second order accurate. Both algorithms are accelerated to the steady state solution using a spatially variable time step procedure. This technique has proved excellent gains in terms of convergence ratio as reported in Maciel. The algorithms are applied to the solution of the steady state physical problem of the supersonic flow along a compression corner. In this paper, the second paper of this series (RESULTS), the numerical solutions obtained with both schemes, in their first and second order accuracies, are presented and analyzed. The results have shown that the Radespiel and Kroll scheme using Barth and Jespersen, Van Leer, Van Albada and Superbee nonlinear limiters presents the most accurate values to the shock angle of the oblique shock wave generated at the compression corner.*

Keywords*: Liou and Steffen Jr. algorithm, Radespiel and Kroll algorithm, Unstructured algorithms, Linear reconstruction, Euler equations.*

1. INTRODUCTION

Conventional non-upwind algorithms have been used extensively to solve a wide variety of problems (Kutler, 1975, and Steger, 1978). Conventional algorithms are somewhat unreliable in the sense that for every different problem (and sometimes, every different case in the same class of problems) artificial dissipation terms must be specially tuned and judicially chosen for convergence. Also, complex problems with shocks and steep compression and expansion gradients may defy solution altogether.

Upwind schemes are in general more robust but are also more involved in their derivation and application. Some upwind schemes that have been applied to the Euler equations are the Liou and Steffen Jr. (1993) and the Radespiel and Kroll (1995) ones. These algorithms are described in details in Maciel (2009).

Algorithms for solving the Euler equations using a perfect gas model on structured grids in two and three dimensions have become widespread in recent years (Turkel and Van Leer, 1984, and Riggins, Walters and Pelletier, 1988). However, these algorithms have shown difficulties in predicting satisfactory results around complex geometries due to mesh irregularities. As a result, attention has turned to the development of solution algorithms on arbitrary unstructured grids. Impressive results have been obtained for a wide range of problems (Mavriplis and Jameson, 1987, and Barth and Jespersen, 1989).

One problem associated with unstructured meshes is the increased difficulty in obtaining smooth higher order spatial approximations to state data at cell interfaces. Two methods have been used to obtain higher order accuracy on unstructured meshes. A method used by several researchers for cell vertex schemes (Stoufflet *et al*., 1987, and Whitaker, 1988) was applied to obtain higher order accuracy in a procedure analogous to MUSCL differencing on a structured mesh. A conventional structured mesh limiter can be employed in this scheme to obtain approximately monotone results near flow discontinuities. The second method, which was proposed by Barth and Jespersen (1989), linearly reconstructs the cell averaged data and imposes a monotone preserving limiter to achieve smooth results near flow discontinuities.

On an unstructured algorithm context, Maciel (2007a,b) have presented a work involving the numerical implementation of four typical algorithms of the Computational Fluid Dynamics community. The Roe (1981), the Steger and Warming (1981), the Van Leer (1982) and the Harten (1983) algorithms were implemented and applied to the solution of aeronautical and of aerospace problems, in two-dimensions. The Euler equations in conservative form, employing a finite volume formulation and an unstructured spatial discretization, were solved. More comments of this work are reported in Maciel (2009).

Following the studies of 2007, Maciel (2008a,b) have presented a work involving the numerical implementation of more three typical algorithms of the Computational Fluid Dynamics community. The Frink, Parikh and Pirzadeh

(1991), the Liou and Steffen Jr. (1993), and the Radespiel and Kroll (1995) algorithms were implemented and applied to the solution of aeronautical and aerospace problems, in two-dimensions. The Euler equations in conservative form, employing a finite volume formulation and an unstructured spatial discretization, were solved. More comments of this work are reported in Maciel (2009).

In the present work, the Liou and Steffen Jr. (1993) and the Radespiel and Kroll (1995) schemes are implemented, on a finite volume context and using an upwind and unstructured spatial discretization, to solve the Euler equations in the two-dimensional space. Both schemes are flux vector splitting ones. These schemes are implemented in their second order accuracy versions employing the reconstruction linear method of Barth and Jespersen (1989) and their results are compared with their first order accuracy versions and with theoretical results. Five nonlinear flux limiters are studied: Barth and Jespersen (minmod like), Van Leer, Van Albada, Superbee and β-limiter. The time integration uses a Runge-Kutta method of five stages and is second order accurate. Both algorithms are accelerated to the steady state solution using a spatially variable time step. This technique has proved excellent gains in terms of convergence ratio as reported in Maciel (2005 and 2008c). The algorithms are applied to the solution of the steady state physical problem of the supersonic flow along a compression corner.

In this paper, the second part of this series (RESULTS), the numerical solutions obtained with both schemes, in their first and second order accuracies, are presented and analyzed. The results have shown that the Radespiel and Kroll (1995) scheme using Barth and Jespersen, Van Leer, Van Albada and Superbee nonlinear limiters presents the most accurate values to the shock angle of the oblique shock wave generated at the compression corner.

An unstructured discretization of the calculation domain is usually recommended to complex configurations, due to the easily and efficiency that such domains can be discretized (Mavriplis, 1990, and Pirzadeh, 1991). However, the unstructured mesh generation question will not be studied in this work.

2. RESULTS

Tests were performed in a microcomputer with processor INTEL CELERON, 1.5GHz of “clock”, and 1.0Gbyte of RAM. Converged results occurred to four (4) orders of reduction in the maximum residual value. The entrance angle is equal to 0.0° for the compression corner problem. The ratio of specific heats, γ, assumed the value 1.4. The reference to the limiters is abbreviated in this work: Barth and Jespersen limiter (BJ), Van Leer limiter (VL), Van Albada limiter (VA), Superbee limiter (SB) and β-limiter (BL).

2.1. Compression corner problem – Qualitative analyses

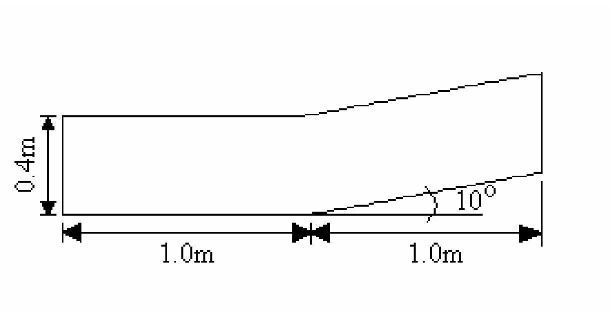

Figure 1. Compression corner configuration.

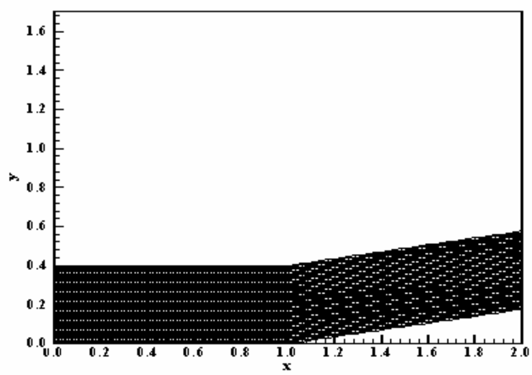

Figure 2. Compression corner mesh.

The compression corner configuration is described in Fig. 1. The corner inclination angle is 10^{o}. An algebraic mesh of 70x50 points or composed of 3,381 rectangular cells and 3,500 nodes was initially generated. Later, the connectivity, the neighboring, the nodes, and the ghost tables were constructed to yield a mesh of triangles, composed of 6,762 cells and 3,500 nodes. This mesh is shown in Fig. 2.

Figure 3 exhibits the pressure contours obtained by the first order accuracy version of the Liou and Steffen Jr. (1993) scheme. Figures 4 to 6 show the second order accuracy versions of the Liou and Steffen Jr. (1993) scheme. Figures 4 to 6 show the solutions obtained by the BJ, VL, and VA nonlinear limiters, respectively. The SB and BL limiters did not yield converged solutions. As can be observed from the second order solutions, they present pressure oscillations, which damage the uniformity of the solutions. As can also be noted, the second order versions of the Liou and Steffen Jr. (1993) scheme present smaller oblique shock wave thickness than the first order version, as expected. The second order version of the Liou and Steffen Jr. (1993) scheme employing the VA nonlinear limiter presents the most severe pressure field.

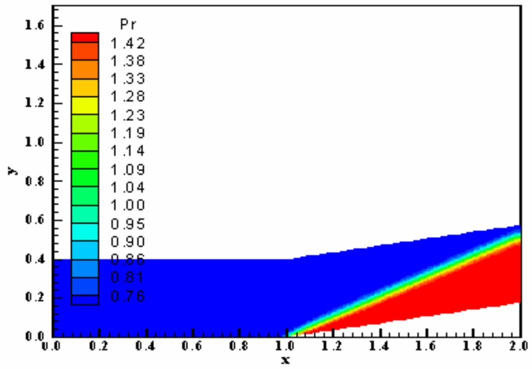

Figure 3. Pressure contours (LS/1a).

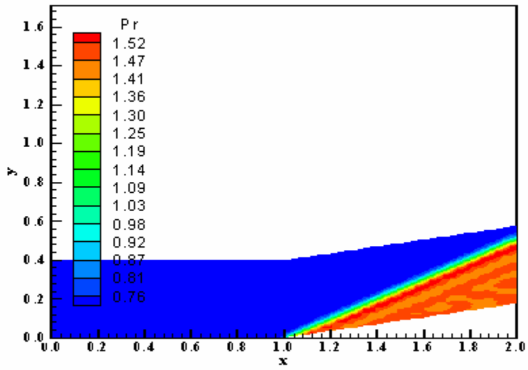

Figure 4. Pressure contours (LS/2a/BJ).

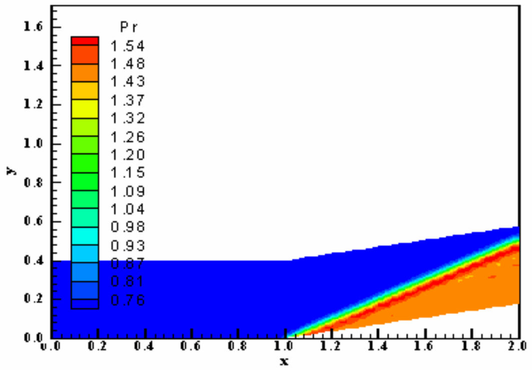

Figure 5. Pressure contours (LS/2a/VL).

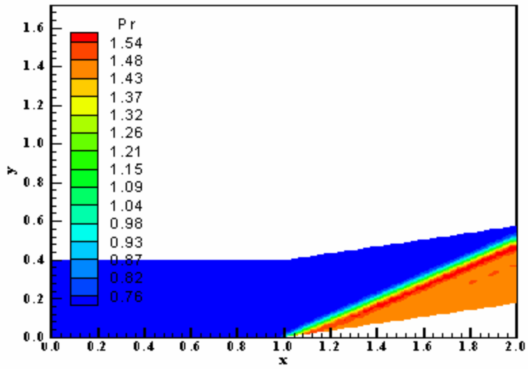

Figure 6. Pressure contours (LS/2a/VA).

Figure 7 exhibits the Mach number contours obtained by the first order accuracy version of the Liou and Steffen Jr. (1993) scheme. Figures 8 to 10 show the second order accuracy versions of the Liou and Steffen Jr. (1993) scheme. Figures 8 to 10 show the solutions obtained by the BJ, VL, and VA nonlinear limiters, respectively. As can be observed from the second order solutions, they present Mach number oscillations, which damage the uniformity of the solutions. As can also be noted, the second order versions of the Liou and Steffen Jr. (1993) scheme present smaller oblique shock wave thickness than the first order version, as expected. The second order version of the Liou and Steffen Jr. (1993) scheme employing the VL nonlinear limiter presents the most intense Mach number field.

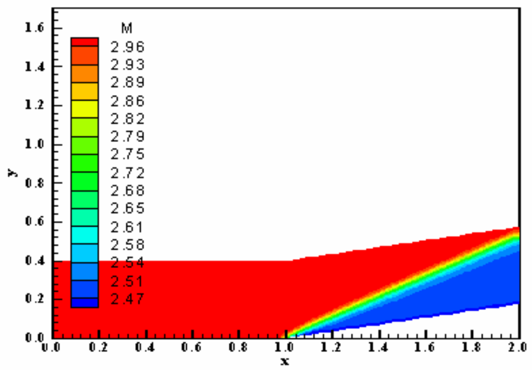

Figure 7. Mach number contours (LS/1a).

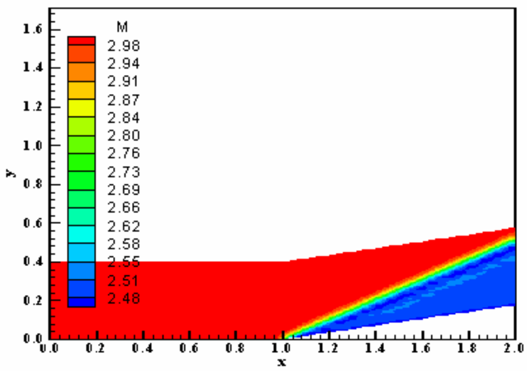

Figure 8. Mach number contours (LS/2a/BJ).

Figure 11 exhibits the wall pressure distributions obtained by the first and second order versions of the Liou and Steffen Jr. (1993) scheme using symbols to illustrate in how many cells these versions capture the shock discontinuity. They are compared with the oblique shock wave theory results. As can be observed, the first order solution of the Liou and Steffen Jr. (1993) scheme is smooth, without pressure oscillations, capturing the pressure discontinuity in four cells. On the other hand, all second order version solutions of the Liou and Steffen Jr. (1993) scheme present oscillations at the corner, originating a pressure peak, which damages the quality of the solution. Figure 12 shows the wall pressure distributions obtained by the second order versions of the Liou and Steffen Jr. (1993) scheme again using symbols to illustrate in how many cells these versions capture the shock discontinuity. As noted, these versions of the Liou and Steffen Jr. (1993) scheme capture the shock discontinuity using three cells, which is a good result in terms of second order schemes.

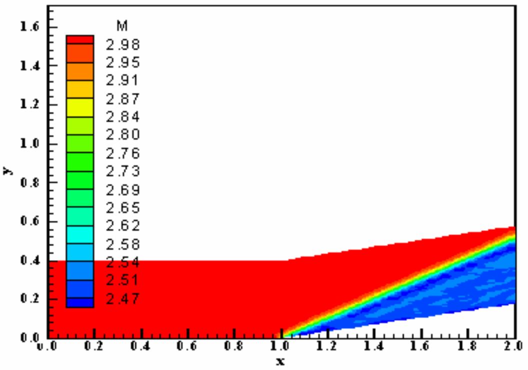

Figure 9. Mach number contours (LS/2a/VL).

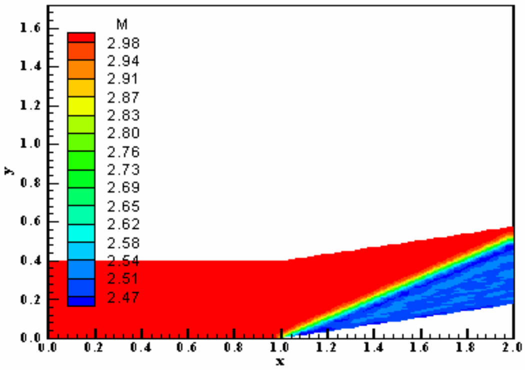

Figure 10. Mach number contours (LS/2a/VA).

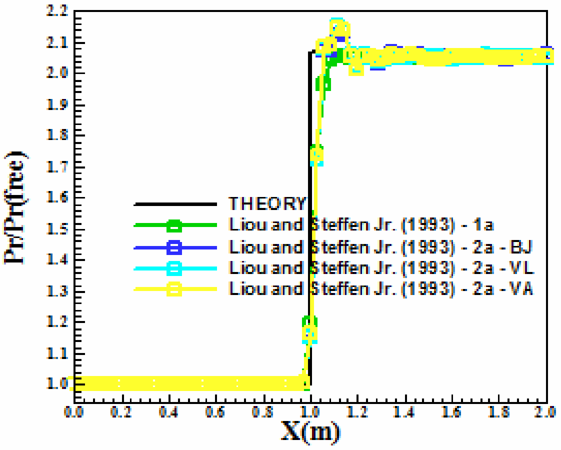

Figure 11. Wall pressure distributions (LS1).

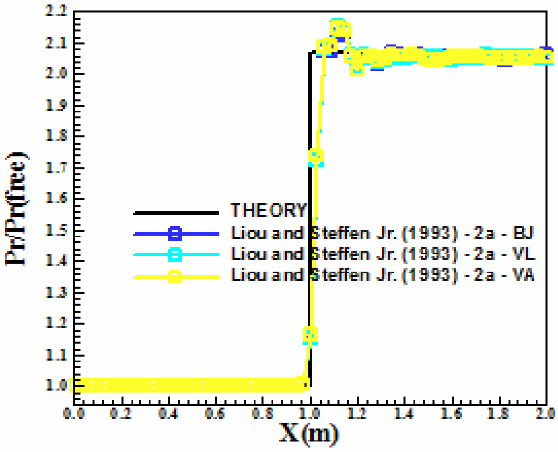

Figure 12. Wall pressure distributions (LS2).

Figure 13 exhibits the pressure contours obtained by the Radespiel and Kroll (1995) scheme in its first order version. Figures 14 to 18 show the pressure contours obtained by the BJ, VL, VA, SB, and BL nonlinear limiters. As can be observed, the BJ, VA, and BL second order solutions of the Radespiel and Kroll (1995) scheme present an oblique shock wave thickness smaller than those obtained by the first order version and by the VL and SB second order versions of the Radespiel and Kroll (1995) scheme. The former solutions also present small pressure oscillations, which did not damage the solution quality. The most severe pressure fields are also obtained by the BJ, VA, and BL second order versions of the Radespiel and Kroll (1995) scheme.

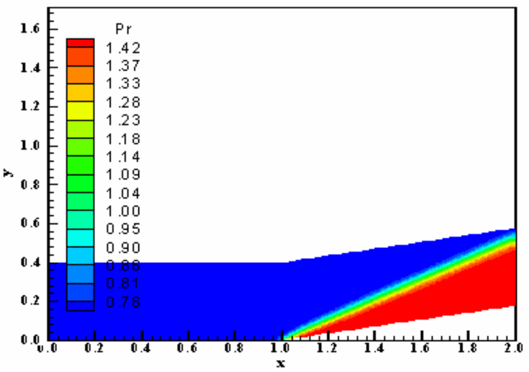

Figure 13. Pressure contours (RK/1a).

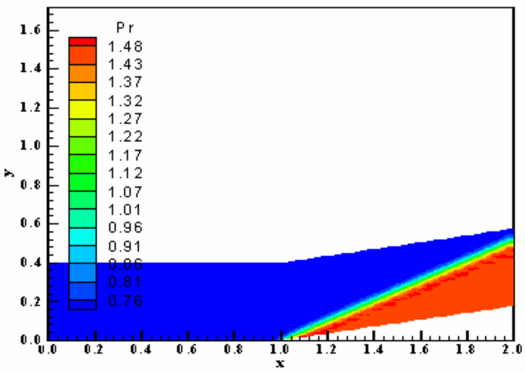

Figure 14. Pressure contours (RK/2a/BJ).

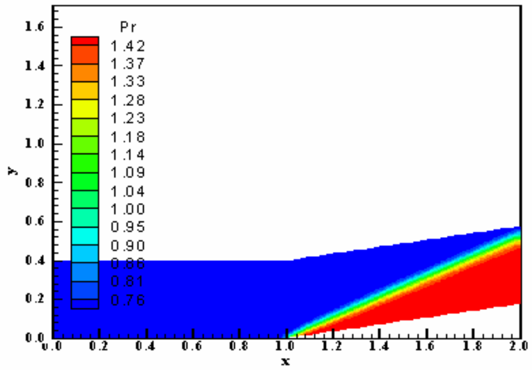

Figure 15. Pressure contours (RK/2a/VL).

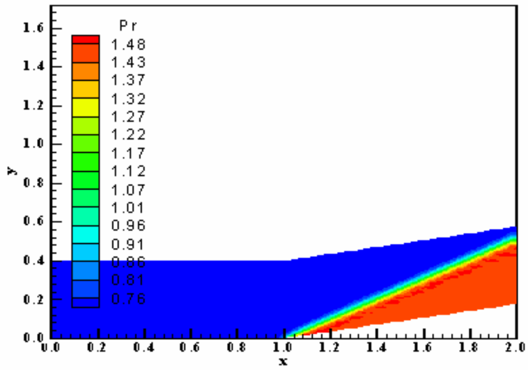

Figure 16. Pressure contours (RK/2a/VA).

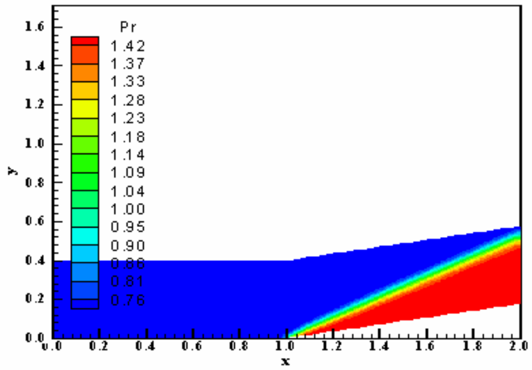

Figure 17. Pressure contours (RK/2a/SB).

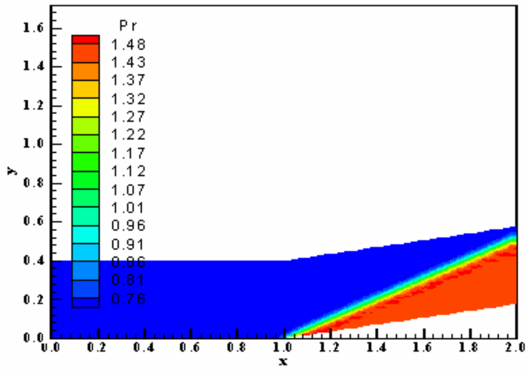

Figure 18. Pressure contours (RK/2a/BL).

Figure 19 exhibits the Mach number contours obtained by the Radespiel and Kroll (1995) scheme in its first order version. Figures 20 to 24 show the Mach number contours obtained by the BJ, VL, VA, SB, and BL nonlinear limiters. As can be observed, all second order solutions of the Radespiel and Kroll (1995) scheme present an oblique shock wave thickness smaller than that obtained by the first order version of the Radespiel and Kroll (1995) scheme. A behavior somewhat different from the pressure contour analyze. The most significant results should be considered the pressure solutions because represent the reference variable to aerospace vehicle design (the pressure). All solutions present small Mach number oscillations, which did not severely damage the solution quality. The most intense Mach number field is obtained by the SB second order version of the Radespiel and Kroll (1995) scheme.

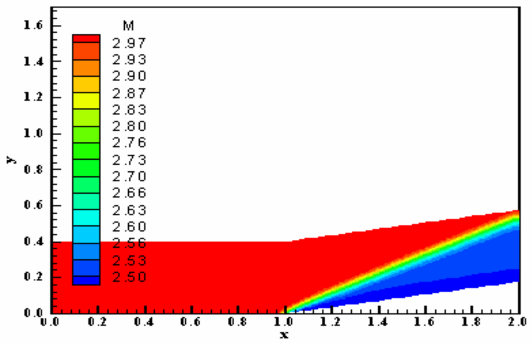

Figure 19. Mach number contours (RK/1a).

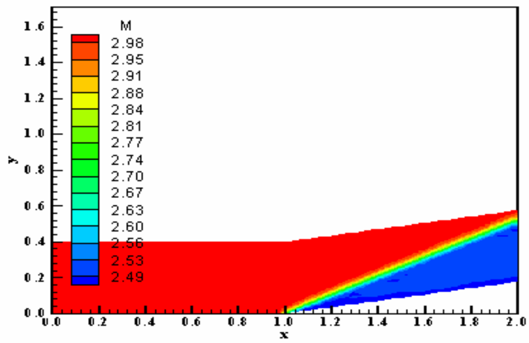

Figure 20. Mach number contours (RK/2a/BJ).

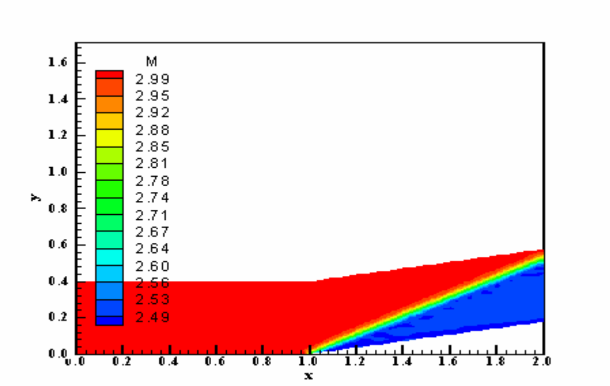

Figure 21. Mach number contours (RK/2a/VL).

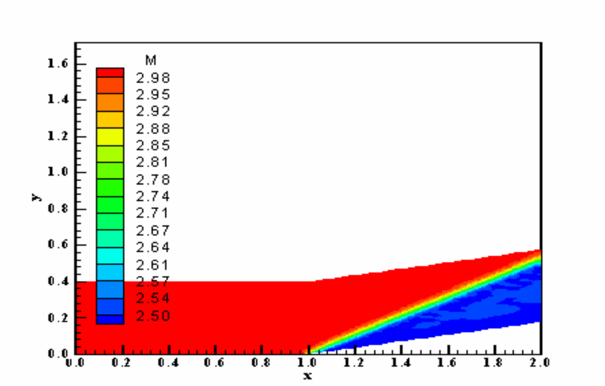

Figure 22. Mach number contours (RK/2a/VA).

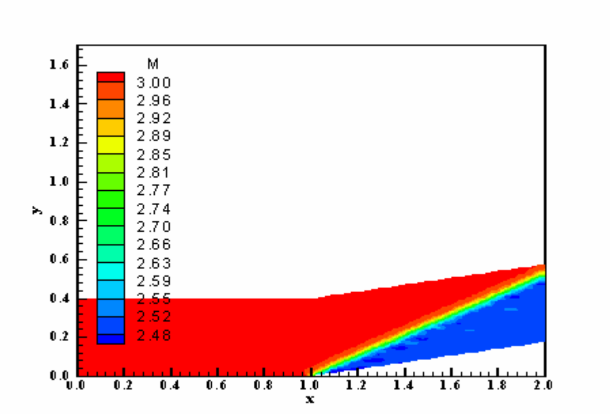

Figure 23. Mach number contours (RK/2a/SB).

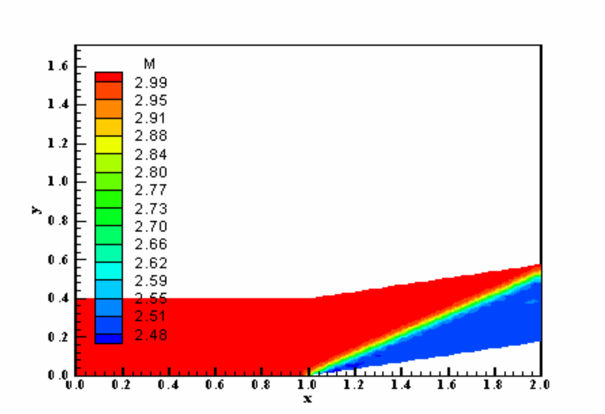

Figure 24. Mach number contours (RK/2a/BL).

Figure 25 shows the wall pressure distributions obtained by the first and second order versions of the Radespiel and Kroll (1995) scheme. They are compared with the oblique shock wave theory results. As observed, the first order version of the Radespiel and Kroll (1995) scheme presents a smooth and oscillation-free wall pressure profile. The shock is captured in four cells. All second order wall pressure profiles of the Radespiel and Kroll (1995) scheme present oscillations at the corner. The second order wall pressure profile generated by the VA nonlinear limiter is better than the others. Figure 26 exhibits the wall pressure distributions generated by the second order versions of the Radespiel and Kroll (1995) scheme using BJ, VL, and VA nonlinear limiters. The shock discontinuity is captured within four cells. Figure 27 shows the wall pressure distributions obtained by the SB and BL nonlinear limiters. The pressure oscillations at the corner for these two limiters are bigger than for the BJ, VL, and VA nonlinear limiters. The shock discontinuity is also captured within four cells. With these results, it is possible to conclude that the Liou and Steffen Jr. (1993) scheme captures more accurately the shock discontinuity than the Radespiel and Kroll (1995) scheme, considering their second order versions. Figure 28 exhibits the best wall pressure distribution, among all second order versions of the Liou and Steffen Jr. (1993) and of the Radespiel and Kroll (1995) schemes, obtained by the Radespiel and Kroll (1995) scheme using VA limiter.

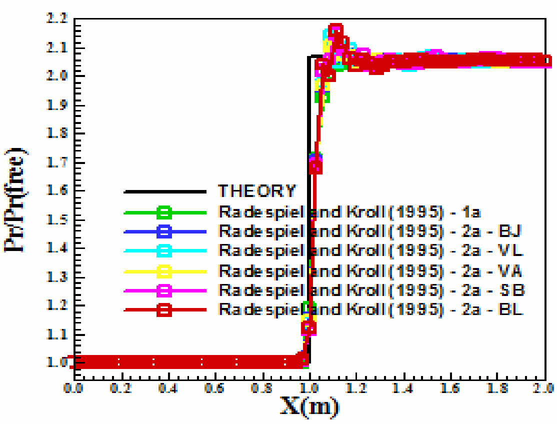

Figure 25. Wall pressure distributions (RK1).

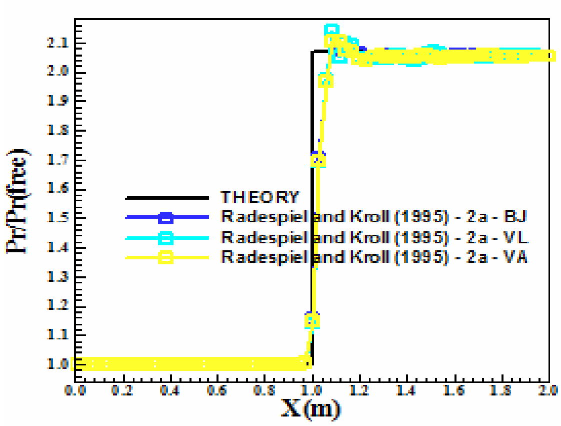

Figure 26. Wall pressure distributions (RK2).

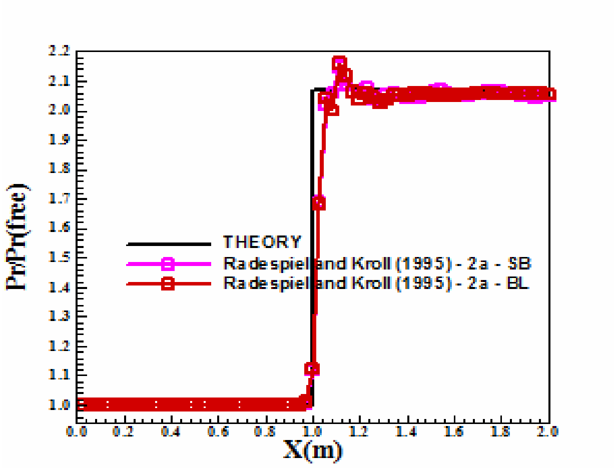

Figure 27. Wall pressure distributions (RK3).

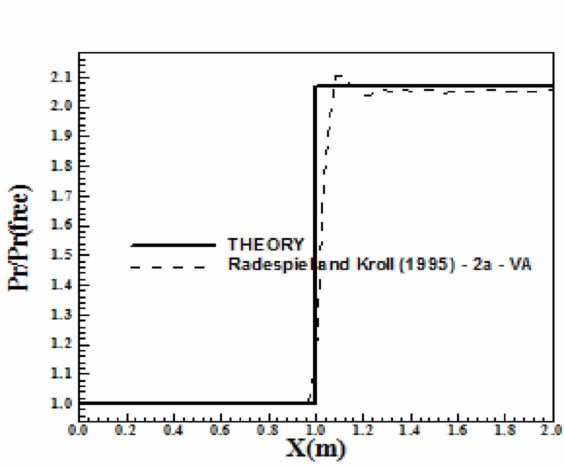

Figure 28. Wall pressure distributions (RK4).

2.2. Compression corner problem – Quantitative analyses – Shock angle of the oblique shock wave and computational costs

One way to quantitatively verify if the solutions generated by each scheme are satisfactory consists in determining the shock angle of the oblique shock wave, β, measured in relation to the initial direction of the flow field. Anderson Jr. (1984) (pages 352 and 353) presents a diagram with values of the shock angle, β, to oblique shock waves. The value of this angle is determined as function of the freestream Mach number and of the deflection angle of the flow after the shock wave, ϕ. To the compression corner problem, ϕ = 10º (ramp inclination angle) and the freestream Mach number is 3.0, resulting from this diagram a value to β equals to 27.5º.

Using a transfer in Figures 3 to 6 (pressure contours), it is possible to obtain the values of β to each variant of the Liou and Steffen Jr. (1993) scheme, as well the respective errors, shown in Tab. 1. The Liou and Steffen Jr. (1993) scheme using the BJ limiter has yielded the best result, with an error of 0.36%. The results obtained with the Liou and Steffen Jr. (1993) scheme presented a maximum error less than 1.10%, but none of them presented an exact value to the shock angle.

Table 1. Shock angle of the oblique shock wave and percentage error (LS).

Algorithm	β(°)	Error (%)
Liou and Steffen Jr. (1993) – 1a	27.8	1.09
Liou and Steffen Jr. (1993) – 2a – BJ	27.4	0.36
Liou and Steffen Jr. (1993) – 2a – VL	27.8	1.09
Liou and Steffen Jr. (1993) – 2a – VA	27.2	1.09

Using now a transfer in Figures 13 to 18 (pressure contours), it is possible to obtain the values of β to each variant of the Radespiel and Kroll (1995) scheme, as well the respective errors, shown in Tab. 2. The Radespiel and Kroll (1995) scheme using the BJ, VL, VA, and SB limiters have yielded the exact values to the shock angle, with error of 0.00%. The results obtained with the Radespiel and Kroll (1995) scheme presented a maximum error less than 3.30%, but four solutions presented exact values to the shock angle.

Table 2. Shock angle of the oblique shock wave and percentage error (RK).

Algorithm	β(°)	Error (%)
Radespiel and Kroll (1995) – 1a	28.4	3.27
Radespiel and Kroll (1995) – 2a – BJ	27.5	0.00
Radespiel and Kroll (1995) – 2a – VL	27.5	0.00
Radespiel and Kroll (1995) – 2a – VA	27.5	0.00
Radespiel and Kroll (1995) – 2a – SB	27.5	0.00
Radespiel and Kroll (1995) – 2a – BL	27.7	0.73

Table 3 presents the computational costs of the algorithms of Liou and Steffen Jr. (1993) and of Radespiel and Kroll (1995) in their first and second order versions. Considering only the second order versions of each algorithm, the most expensive is the scheme of Radespiel and Kroll (1995) using the VA limiter, whereas the cheapest is due to Liou and

Steffen Jr. (1993) using BJ limiter. The Liou and Steffen Jr. (1993) algorithm using the BJ limiter is 12.5% cheaper than the Radespiel and Kroll (1995) algorithm using the VA limiter.

Table 3. Computational cost of the numerical algorithms.

Algorithm	Cost(1)
Liou and Steffen Jr. (1993) – 1a	0.0000201
Liou and Steffen Jr. (1993) – 2a – BJ	0.0001096
Liou and Steffen Jr. (1993) – 2a – VL	0.0001224
Liou and Steffen Jr. (1993) – 2a – VA	0.0001227
Radespiel and Kroll (1995) – 1a	0.0000207
Radespiel and Kroll (1995) – 2a – BJ	0.0001108
Radespiel and Kroll (1995) – 2a – VL	0.0001220
Radespiel and Kroll (1995) – 2a – VA	0.0001233
Radespiel and Kroll (1995) – 2a – SB	0.0001189
Radespiel and Kroll (1995) – 2a – BL	0.0001182

(1): Measured in seconds/per cell/per iteration.

3. CONCLUSIONS

In the present work, the Liou and Steffen Jr. (1993) and the Radespiel and Kroll (1995) schemes are implemented, on a finite volume context and using an upwind and unstructured spatial discretization, to solve the Euler equations in the two-dimensional space. Both schemes are flux vector splitting ones. These schemes are implemented in their second order accuracy versions employing the reconstruction linear method of Barth and Jespersen (1989) and their results are compared with their first order accuracy versions and with theoretical results. Five nonlinear flux limiters are studied: Barth and Jespersen (minmod like), Van Leer, Van Albada, Superbee and β-limiter. The time integration uses a Runge-Kutta method of five stages and is second order accurate. Both algorithms are accelerated to the steady state solution using a spatially variable time step. This technique has proved excellent gains in terms of convergence ratio as reported in Maciel (2005 and 2008c). The algorithms are applied to the solution of the steady state physical problem of the supersonic flow along a compression corner.

The results have shown that the Radespiel and Kroll (1995) scheme using Barth and Jespersen, Van Leer, Van Albada, and Superbee nonlinear limiters presents the most accurate values to the shock angle of the oblique shock wave generated at the compression corner. The most severe pressure field generated by the Liou and Steffen Jr. (1993) scheme was obtained when using the VA nonlinear limiter, whereas the Radespiel and Kroll (1995) scheme presented the most severe pressure field when using BJ, VA and BL nonlinear limiters. Moreover, the most intense Mach number field generated by the Liou and Steffen Jr. (1993) scheme was obtained when using the VL nonlinear limiter, whereas the Radespiel and Kroll (1995) scheme presented the most intense Mach number field when using SB nonlinear limiter. In terms of pressure contours – the reference variable to aerospace vehicle design – the second order versions of the Liou and Steffen Jr. (1993) scheme present smaller shock wave thickness than the first order version. Still in terms of pressure contours, the Radespiel and Kroll (1995) scheme using BJ, VA and BL nonlinear limiters detects smaller shock wave thickness than the first order version of this algorithm. These nonlinear limiters also yield smaller shock wave thickness than the Radespiel and Kroll (1995) scheme using VL and SB nonlinear limiters. The wall pressure distributions of both schemes, in their second order versions, present oscillations at the corner, characterizing a pressure peak at this region. The most acceptable solution was due to Radespiel and Kroll (1995) using VA nonlinear limiter. The Liou and Steffen Jr. (1993) scheme, in its second order versions, captures the shock discontinuity using three cells, whereas the Radespiel and Kroll (1995) scheme, in its second order versions, captures the shock discontinuity in four cells. This means that the Liou and Steffen Jr. (1993) scheme is better than the Radespiel and Kroll (1995) scheme in terms of capturing the shock discontinuity. The shock angle of the oblique shock wave is exactly determined by the Radespiel and Kroll (1995) scheme using BJ, VL, VA and SB nonlinear limiters, with an error of 0.00%, whereas only the Liou and Steffen Jr. (1993) scheme using BJ nonlinear limiter presents the closest solution, with an error of 0.36%.

In terms of computational cost, considering only the second order versions of each algorithm, the most expensive is the scheme of Radespiel and Kroll (1995) using the VA limiter, whereas the cheapest is due to Liou and Steffen Jr. (1993) using BJ limiter. The Liou and Steffen Jr. (1993) algorithm using the BJ limiter is 12.5% cheaper than the Radespiel and Kroll (1995) algorithm using the VA limiter, which is a negligible difference.

4. ACKNOWLEDGEMENTS

The author thanks the financial support conceded by CNPq under process number PDJ 150143/2008-7.

5. REFERENCES

Anderson Jr., J. D., 1984, "Fundamentals of Aerodynamics", McGraw-Hill, Inc., EUA, 563p.

Barth, T. J., and Jespersen, D. C., 1989, "The Design and Application of Upwind Schemes on Unstructured Meshes", AIAA Paper 89-0336.

Frink, N. T., Parikh, P., and Pirzadeh, S., 1991, "Aerodynamic Analysis of Complex Configurations Using Unstructured Grids", AIAA 91-3292-CP.

Harten, A., 1983, "High Resolution Schemes for Hyperbolic Conservation Laws", Journal of Computational Physics, Vol. 49, pp. 357-393.

Kutler, P., 1975, "Computation of Three-Dimensional, Inviscid Supersonic Flows", Lecture Notes in Physics, Vol. 41, pp. 287-374.

Liou, M., and Steffen Jr., C. J., 1993, "A New Flux Splitting Scheme", Journal of Computational Physics, Vol. 107, pp. 23-39.

Maciel, E. S. G., 2005, "Analysis of Convergence Acceleration Techniques Used in Unstructured Algorithms in the Solution of Aeronautical Problems – Part I", Proceedings of the XVIII International Congress of Mechanical Engineering (XVIII COBEM), Ouro Preto, MG, Brazil.

Maciel, E. S. G., 2007a, "Comparison Between the First Order Upwind Unstructured Algorithms of Roe and of Harten in the Solution of the Euler Equations in Two-Dimensions", Proceedings of the XIX Congress of Mechanical Engineering (XIX COBEM), Brasília, DF, Brazil.

Maciel, E. S. G., 2007b, "Comparison Between the First Order Upwind Unstructured Algorithms of Steger and Warming and of Van Leer in the Solution of the Euler Equations in Two-Dimensions", Proceedings of the XIX Congress of Mechanical Engineering (XIX COBEM), Brasília, DF, Brazil.

Maciel, E. S. G., 2008a, "Comparison Among the Unstructured Algorithms of Frink, Parikh and Pirzadeh, of Liou and Steffen, and of Radespiel and Kroll in the Solution of the Euler Equations in 2D - Theory", Proceedings of the 8th Symposium of Computational Mechanics (VIII SIMMEC), Belo Horizonte, MG, Brasil.

Maciel, E. S. G., 2008b, "Comparison Among the Unstructured Algorithms of Frink, Parikh and Pirzadeh, of Liou and Steffen, and of Radespiel and Kroll in the Solution of the Euler Equations in 2D - Results", Proceedings of the 8th Symposium of Computational Mechanics (VIII SIMMEC), Belo Horizonte, MG, Brasil.

Maciel, E. S. G., 2008c, "Analysis of Convergence Acceleration Techniques Used in Unstructured Algorithms in the Solution of Aerospace Problems – Part II", Proceedings of the XII Brazilian Congress of Thermal Engineering and Sciences (XII ENCIT), Belo Horizonte, MG, Brazil.

Maciel, E. S. G., 2009, "Extension of the Unstructured Algorithms of Liou and Steffen Jr. and of Radespiel and Kroll to Second Order Accuracy Employing Linear Reconstruction and Application to the Euler Equations in 2D – Theory", Proceedings of the XX International Congress of Mechanical Engineering (XX COBEM), Gramado, RS, Brazil.

Mavriplis, D. J., 1990, "Accurate Multigrid Solution of the Euler Equations on Unstructured and Adaptive Meshes", AIAA Journal, Vol. 28, No. 2, pp. 213-221.

Mavriplis, D., and Jameson, A., 1987, "Multigrid Solution of the Euler Equations on Unstructured and Adaptive Meshes", ICASE Report. 87-53; also NASA CR 178346.

Pirzadeh, S., 1991, "Structured Background Grids for Generation of Unstructured Grids by Advancing Front Method", AIAA Paper 91-3233-CP.

Radespiel, R., and Kroll, N., 1995, "Accurate Flux Vector Splitting for Shocks and Shear Layers", Journal of Computational Physics, Vol. 121, pp. 66-78.

Riggins, D. W., Walters, R. W., and Pelletier, D., 1988, "The use of Direct Solvers for Compressible Flow Computations", AIAA Paper 88-0229.

Roe, P. L., 1981, "Approximate Riemann Solvers, Parameter Vectors, and Difference Schemes", Journal of Computational Physics, Vol. 43, pp. 357-372.

Steger, J. L., 1978, "Implicit Finite-Difference Simulation of Flow About Arbitrary Two-Dimensional Geometries", AIAA Journal, Vol. 16, No. 7, pp. 679-686.

Steger, J. L. and Warming, R. F., 1981, "Flux Vector Splitting of the Inviscid Gasdynamic Equations with Application to Finite-Difference Methods", Journal of Computational Physics, Vol. 40, pp. 263-293.

Stoufflet, B., Périaux, J., Fezoui, F., and Dervieux, A., 1987, "Numerical Simulation of 3-D Hypersonic Euler Flows Around Space Vehicles Using Adapted Finite-Elements", AIAA Paper 87-0560.

Turkel, E., and Van Leer, B., 1984, "Flux-Vector Splitting and Runge-Kutta Methods for the Euler Equations", ICASE Report 84-27; also NASA CR 172415.

Van Leer, B., 1982, "Flux-Vector Splitting for the Euler Equations", Proceedings of the 8th International Conference on Numerical Methods in Fluid Dynamics, E. Krause, Editor, Lecture Notes in Physics, Vol. 170, pp. 507-512, Springer-Verlag, Berlin.

Whitaker, D. L., 1988, "Two-Dimensional Euler Computations on a Triangular Mesh Using an Upwind, Finite-Volume Scheme", Ph.D. Thesis, Dept. of Aerospace and Ocean Engineering, Virginia Polytechnic Inst. and State Univ., Blacksburg, VA.

6. RESPONSIBILITY NOTICE

The author is the only responsible for the printed material included in this paper.